Electronic Supplementary Material (ESI) for Journal of Materials Chemistry C.
This journal is © The Royal Society of Chemistry 2022

Highly Twisted Bipolar Molecules for Efficient Near-Ultraviolet Organic Light-Emitting Diodes via Hybridized Local and Charge-Transfer Mechanism

Ziting Zhong,[a,‡] Zhangshan Liu, [b,‡] Sinuo Geng,[a] Huihui Li,[a] Xin Jiang Feng,*[,a] Zujin Zhao,*[,b] and Hua Lu*[,a]

I. Supplementary Figures and Tables.

1. **Fig. S1** TGA and DSC traces.....S2
2. **Fig. S2** Absorption spectra of **C2MPI**, **C2PPI** in different solvents.....S2
3. **Fig. S3** Emission spectra of **C2MPI**, **C2PPI** in different solvents.....S2
4. **Table S1** Photophysical properties of **C2MPI**, **C2PPI** in different solvents.....S3
5. **Fig. S4** Emission spectra and pictures of powders @365 nm UV lamp (inset) in film and in powder.....S3
6. **Table S2** Emission band maxima and the absolute quantum yields in the solid-state.....S3
7. **Fig. S5** Configurations and the twisting angles of **C2MPI** and **C2PPI** by theoretical calculation.....S4
8. **Fig. S6** Natural transition orbitals of S_0 to S_n/T_n for **C2MPI** and **C2PPI**.....S4
9. **Table S3** TD-DFT calculation using the B3LYP functional with 6-31G(d,p) basis sets.....S5
10. **Fig. S7** Doped device configuration, molecules used and their energy levels.....S6
11. **Fig. S8** Luminance-voltage-current density characteristics for devices B1−B8.....S7
12. **Fig. S9** External quantum efficiencies-luminance characteristics for devices B1−B8.....S7
13. **Fig. S10** EL spectra for devices B1−B8.....S7

II. General details and measurements specifications......S8

III. ^{1}H NMR of **C2MPI**, **C2PPI** in $CDCl_3$ or CD_2Cl_2.....S10

IV. ^{13}C NMR of **C2MPI**, **C2PPI** in $CDCl_3$ or CD_2Cl_2.....S14

V. HR-MS of **C2MPI**, **C2PPI**.....S17

I. Supplementary Figures and Tables.

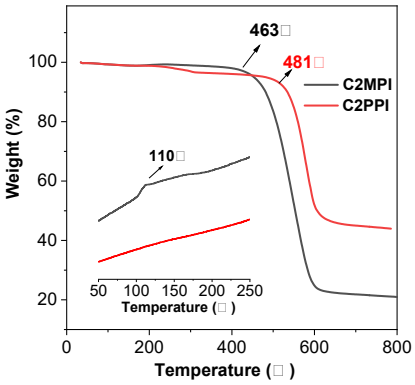

Fig. S1. Thermogravimetric analysis traces differential scanning calorimetry traces (inset) for **C2MPI** and **C2PPI**.

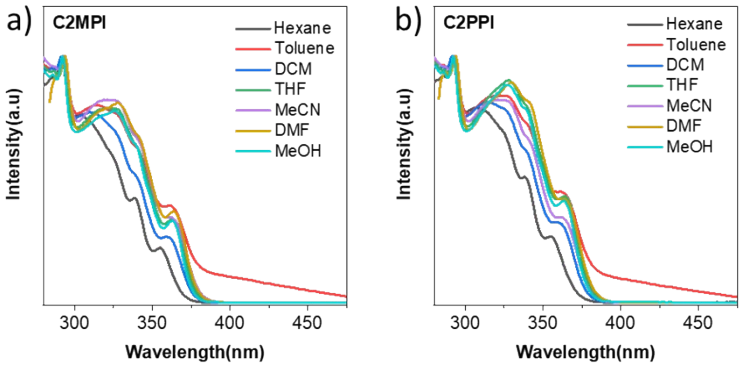

Fig. S2. Absorption spectra of **C2MPI** a) and **C2PPI** b) in different solvents.

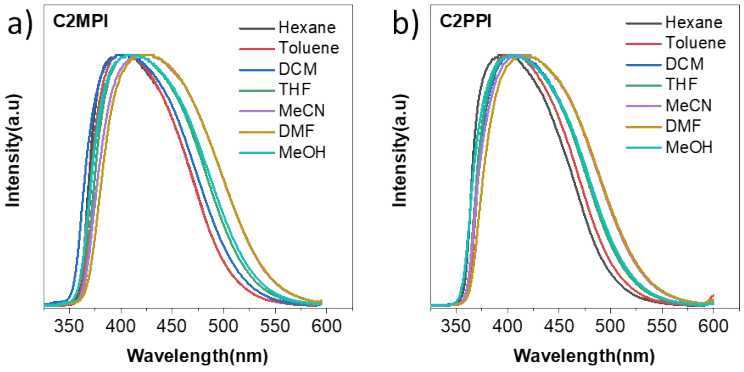

Fig. S3 Emission spectra of **C2MPI** a), **C2PPI** b) in different solvents.

Table S1. Photo physical properties of **C2MPI** and **C2PPI** in different solvents.

	Solvent	λ_{abs} [a] (nm)	λ_{em} [a] (nm)	$\Delta\nu_{em\text{-}abs}$ [b] (cm^{-1})	Φ_F [c]	τ_F [ns] [d]
C2MPI	Hexane	363	398	2423	0.80	1.63
	Toluene	364	402	2597	0.86	0.00
	DCM	363	409	3098	0.86	2.08
	THF	363	407	2978	0.94	1.39
	MeCN	360	413	3565	0.99	1.65
	DMF	362	417	3643	1.00	1.53
	MeOH	355	406	3538	0.99	1.51
C2PPI	Hexane	363	404	2796	0.83	1.21
	Toluene	364	410	3082	0.90	0.00
	DCM	362	415	3528	0.94	1.34
	THF	364	411	3142	1.00	1.38
	MeCN	359	421	4102	1.00	1.48
	DMF	362	425	4095	1.00	1.56
	MeOH	355	411	3838	0.59	1.40

[a] Absorption and emission maxima. [b] Stokes-shift value. [c] Fluorescence quantum yield. [d] Fluorescence lifetime detected at the maximum fluorescence wavelengths.

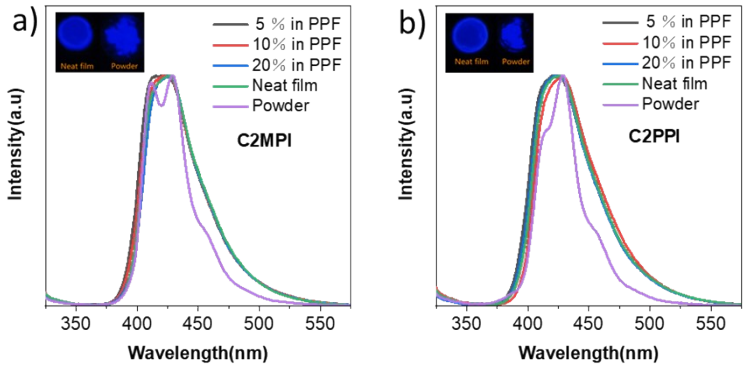

Fig. S4. Emission spectra and pictures of powders @365 nm UV lamp (inset) of **C2MPI** a) and **C2PPI** b) in film and in powder.

Table S2. Emission band maxima and the absolute quantum yields of **C2MPI** and **C2PPI** in the PPF film and in the powder form.

	Film				Powder
E_m/Φ_F	5% in PPF	10% in PPF	20% in PPF	Neat	
C2MPI	422/0.94	424/0.91	425/0.99	427/0.88	429/0.90
C2PPI	420/1.00	428/1.00	425/0.99	426/0.91	428/0.62

PPF = 2,8-bis(diphenylphosphoryl)dibenzo[b,d]furan

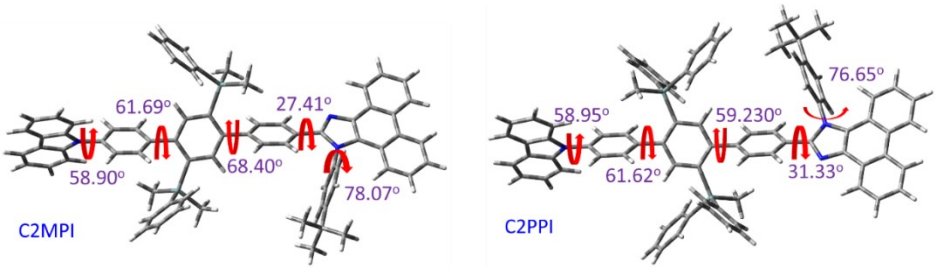

Fig. S5. Configurations and the twisting angles of **C2MPI** and **C2PPI** derived from theoretical calculation.

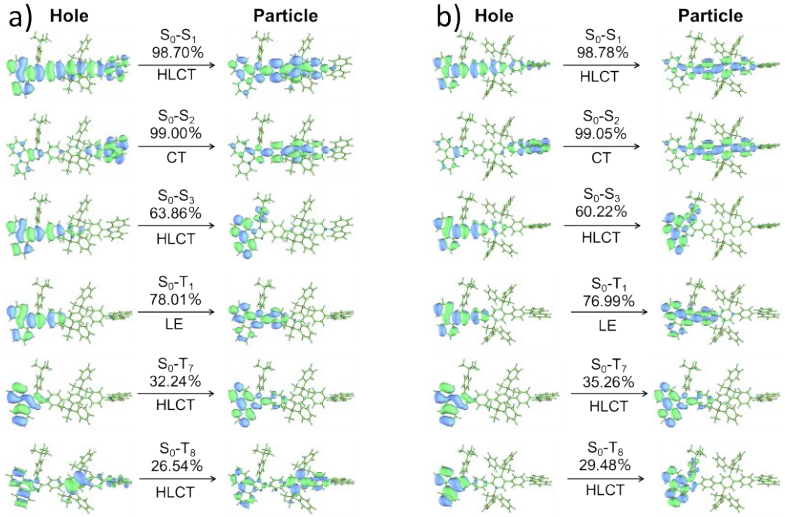

Fig. S6. Natural transition orbitals of S_0 to S_n/T_n for a) **C2MPI** and b) **C2PPI**.

Table S3. Calculated excited wavelength (λ), oscillator strengths (*f*) and the related wave functions calculated by using the B3LYP functional with 6-31G(d,p) basis sets.

	State[a]	E (eV) [b]	λ(nm)[c]	*f* [d]	Orbital (coefficient)[e]
C2MPI	S1	3.73	333	0.9574	H-1→L (36%), H→L (54%)
	S2	3.86	322	0.0311	H-1→L (44%), H→L (31%), H→L+1 (13%)
	S3	3.90	318	0.0260	H-1→L (11%), H-1→L+1 (10%), H-1→L+2 (37%), H→L+2 (25%)
	S4	4.06	306	0.0541	H-1→L+3 (43%), H→L+1 (13%), H→L+3 (24%)
	S5	4.10	303	0.0568	H-1→L+4 (30%), H→L+4 (61%)
	S6	4.11	302	0.0536	H-1→L+1 (18%), H→L (13%), H→L+1 (41%)
	S7	4.16	299	0.0439	H-3→L (14%), H-1→L+5 (37%), H→L+5 (25%)
	S9	4.27	291	0.0205	H-1→L+6 (15%), H→L+5 (13%), H→L+6 (44%)
C2PPI	S1	3.67	339	0.9317	H→L (93%)
	S2	3.82	325	0.0301	H-1→L (85%)
	S5	4.10	303	0.0570	H-1→L+3 (83%)
	S7	4.19	297	0.0441	H-3→L (18%), H→L+6 (49%)
	S8	4.20	296	0.0930	H-1→L+1 (67%)
	S9	4.23	293	0.0361	H-1→L+4 (53%), H-1→L+5 (11%), H→L+4 (11%)

[a)] Excited state. [b)] Calculated energy gaps. [c)] Experimental absorption wavelengths [d)] Oscillator strength (values < 0.02 are not included). [e)] MOs involved in the transitions, H = HOMO, L = LUMO.

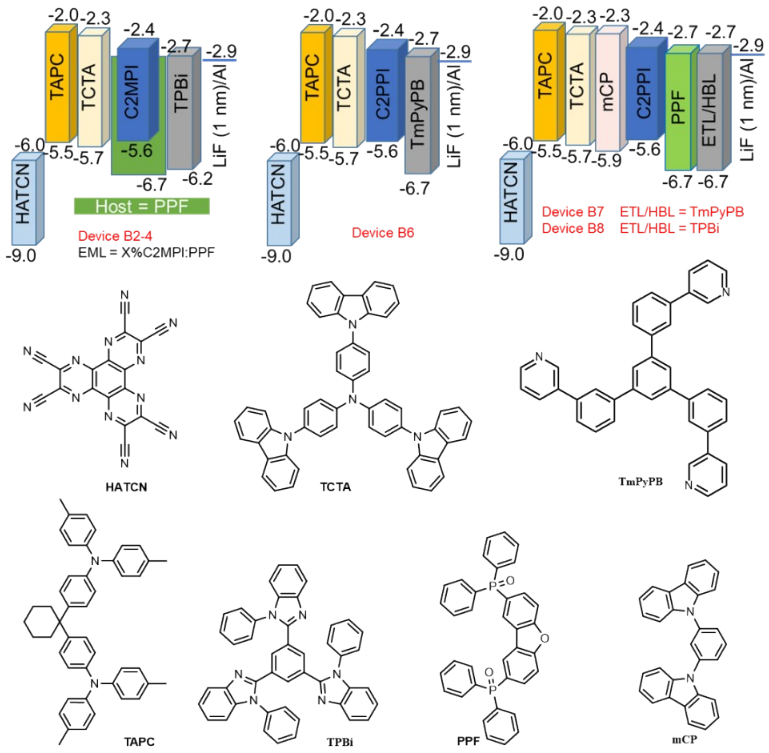

Fig. 7. Device configurations of B2-4 and B6-8, molecules used and their energy levels.

Device configurations and the functional materials used are as follows:

B1: ITO/HATCN (5 nm)/TAPC (60 nm)/TcTa (5 nm)/C2MPI (20 nm) /TPBi (40 nm)/LiF (1 nm)/Al

B2: ITO/HATCN (5 nm)/TAPC (60 nm)/TcTa (5 nm)/5 wt% C2MPI (20 nm): PPF/ TPBi (40 nm)/LiF (1 nm)/Al

B3: ITO/HATCN (5 nm)/TAPC (60 nm)/TcTa (5 nm)/10 wt% C2MPI (20 nm): PPF / TPBi (40 nm)/LiF (1 nm)/Al

B4: ITO/HATCN (5 nm)/TAPC (60 nm)/TcTa (5 nm)/20 wt% C2MPI (20 nm): PPF / TPBi (40 nm)/LiF (1 nm)/Al

B5: ITO/HATCN (5 nm)/TAPC (50 nm)/TcTa (5 nm)/C2PPI (20 nm) /TPBi (40 nm)/LiF (1 nm)/Al

B6: ITO/HATCN (5 nm)/TAPC (50 nm)/TcTa (5 nm)/C2PPI (20 nm) /TmPyPB (40 nm)/LiF (1 nm)/Al

B7: ITO/HATCN (5 nm)/TAPC (50 nm)/TcTa (5 nm)/mCP (5 nm)/C2PPI (20 nm) /PPF (5 nm)/TmPyPB (40 nm)/LiF (1 nm)/Al

B8: ITO/HATCN (5 nm)/TAPC (50 nm)/TcTa (5 nm)/mCP (5 nm)/C2PPI (20 nm) /PPF (5 nm)/TPBi (40 nm)/LiF (1 nm)/Al

ITO: transparent anode; HATCN: hole-injecting layer (HIL); TAPC: hole-transporting layer (HTL); TcTa: electron- and exciton-blocking layer; mCP: works as a buffer layer between hole-transporting layer and light-emitting layer, PPF: exciton blocking layer; TmPyPB/TPBi: electron-transporting layer (ETL) and hole-blocking layer (HBL); LiF and Al: electron-injecting layer (EIL) and cathode.

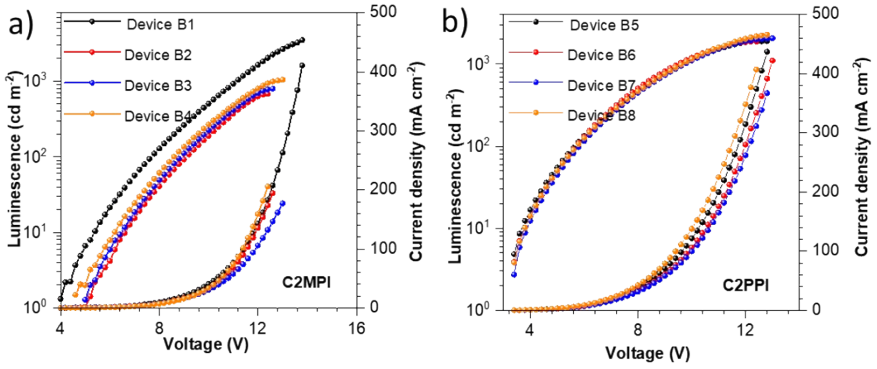

Fig. S8. Luminance-voltage-current density characteristics for devices using **C2MPI** a), **C2PPI** b) as emitters.

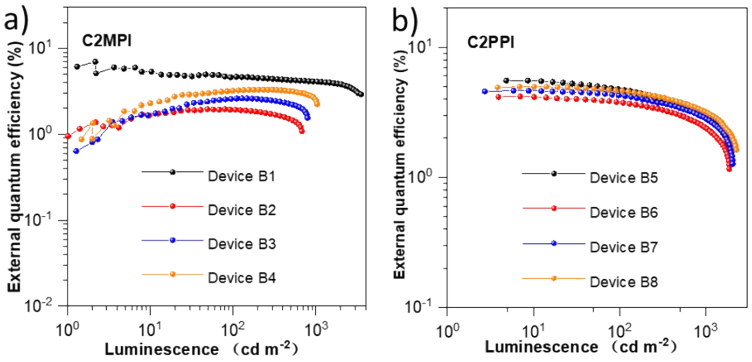

Fig. S9. External quantum efficiencies-luminance characteristics for devices using **C2MPI** a), **C2PPI** b) as emitters.

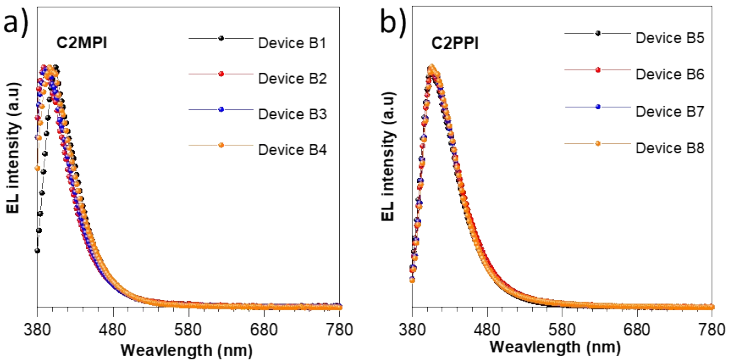

Fig. S10. EL spectra for devices using **C2MPI** a), **C2PPI** b) as emitters.

II. General details and measurement specifications

General details

All reagents and solvents were used as purchased from commercial sources. Toluene and tetrahydrofuran were anhydrous. ^{1}H NMR and ^{13}C NMR spectra, mass spectrometric measurements, thermogravimetric analysis, differential scanning calorimetry (DSC) analysis, UV-Vis spectra, and fluorescence spectra in solution were measured using a Bruker AM 400/500 spectrometer, MicroQII mass spectrometer, TGA instrument (PE-TGA6), TA Instruments DSC 2920, Shimadzu UV-1800 spectrophotometer and Horiba JobinYvon Fluorolog-3 spectrofluorimeter, respectively. The fluorescence quantum yields of the films were measured by the integrating sphere using Hamamatsu C13534 spectrometer. Cyclic voltammetric (CV) measurements were performed using a computer-controlled on a computer-controlled CHI650E.

Spectroscopic measurements

Absorption and emission measurements were carried out in 1 × 1 cm quartz cuvettes. Films were prepared by evaporation of the 2,8-bis(diphenylphosphoryl)dibenzo[b,d]furan (PPF) containing 5 wt%，10 wt% and 20 wt% dyes in dichloromethane onto a Teflon vessel, which was utilized to measure the electronic spectra. These films were stable and no change in absorption and emission was observed over an extended period of time.

The redox potentials were measured on a Zahner Electrochemical Workstation at room temperature with a platinum working electrode, a platinum wire counter electrode, and an Ag/Ag^{+} reference electrode using Fc^{+}/Fc as an external standard and 0.1 M n-Bu_4NPF_6 solution in DCM as a supporting electrolyte.

Device fabrication

Glass substrates pre-coated with a 90 nm-thin layer of indium tin oxide (ITO) with a sheet resistance of 15–20 Ω per square were completely cleaned in ultrasonic bath of detergent and deionized water, respectively, each step takes 30 minutes. After that, the substrates were dried in a 65 ^{o}C oven. Then, the substrates were treated by O_2 plasma for 10 minutes to improve the hole injection capacity of ITO. The vacuum-deposited OLEDs were constructed under a pressure of < 5 × 10^{-4} Pa. Organic materials, LiF and Al were deposited with the rates of 1–2 Å s^{-1}, 0.1 Å s^{-1} and 10 Å s^{-1}, respectively. All the device characterizations were carried out at room temperature under ambient laboratory

conditions without any additional encapsulation, as soon as the devices were fabricated. EL spectra were obtained in normal direction via a spectrometer (Ocean Optics USB 2000+). Current density-voltage-luminance and external quantum efficiency were characterized with a dual-channel Keithley 2614B source meter and a PIN-25D silicon photodiode.

DFT calculations

The G16W software package was used to carry out a DFT geometry optimization using the B3LYP functional with 6-31G(d,p) basis sets. UV-visible spectra were calculated by the B3LYP functional with 6-31G(d,p) basis sets.

III. **^{1}H NMR** of **C2MPI** and **C2PPI** in $CDCl_3$ or CD_2Cl_2.

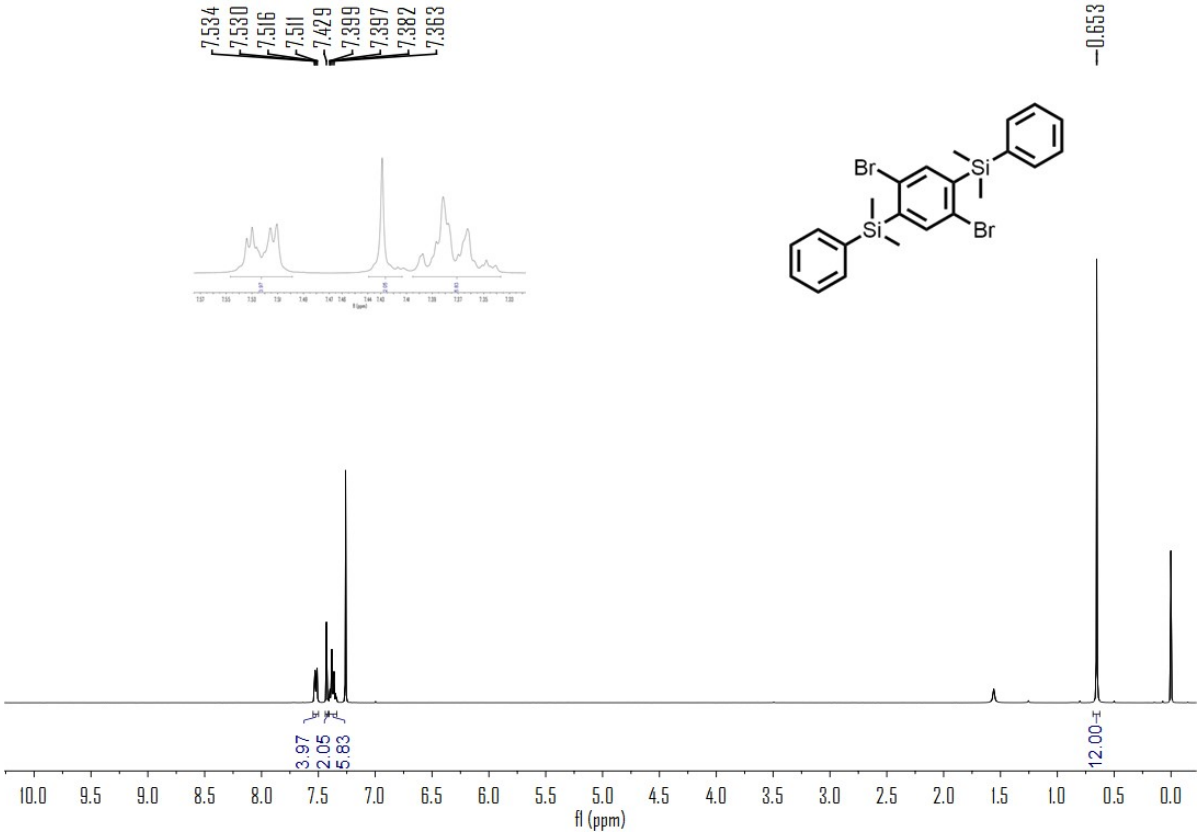

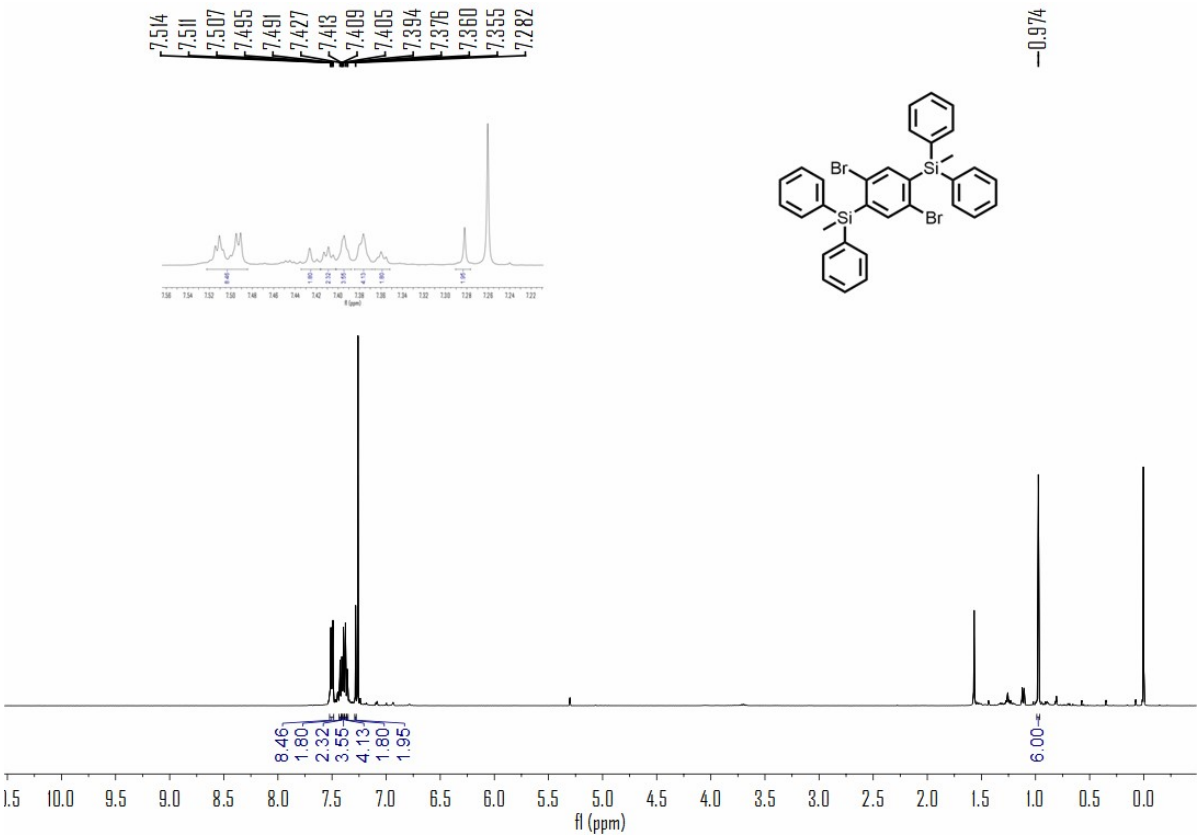

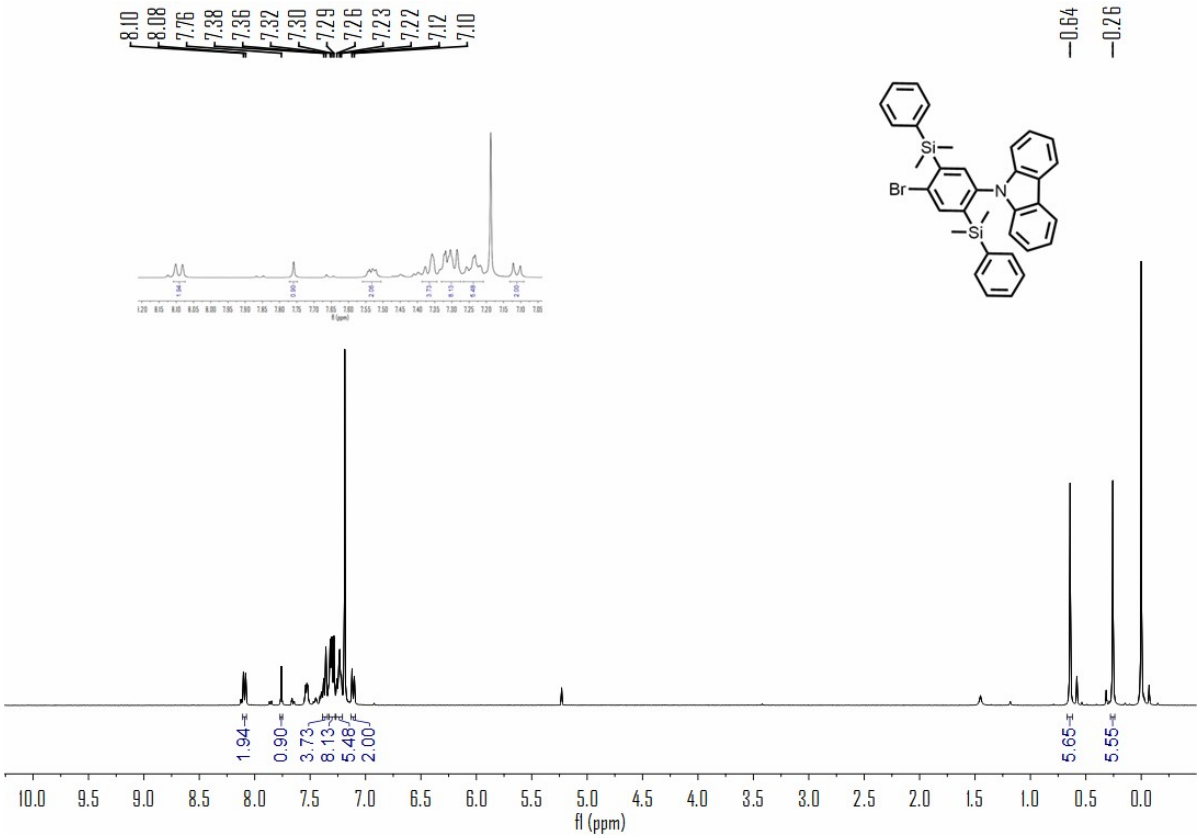
8.10
8.08
7.76
7.38
7.36
7.32
7.30
7.29
7.26
7.23
7.22
7.12
7.10
-0.64
-0.26
Si
Br
N
Si
1.94
0.90
3.73
8.13
5.48
2.00
5.65
5.55
10.0 9.5 9.0 8.5 8.0 7.5 7.0 6.5 6.0 5.5 5.0 4.5 4.0 3.5 3.0 2.5 2.0 1.5 1.0 0.5 0.0
f1 (ppm)

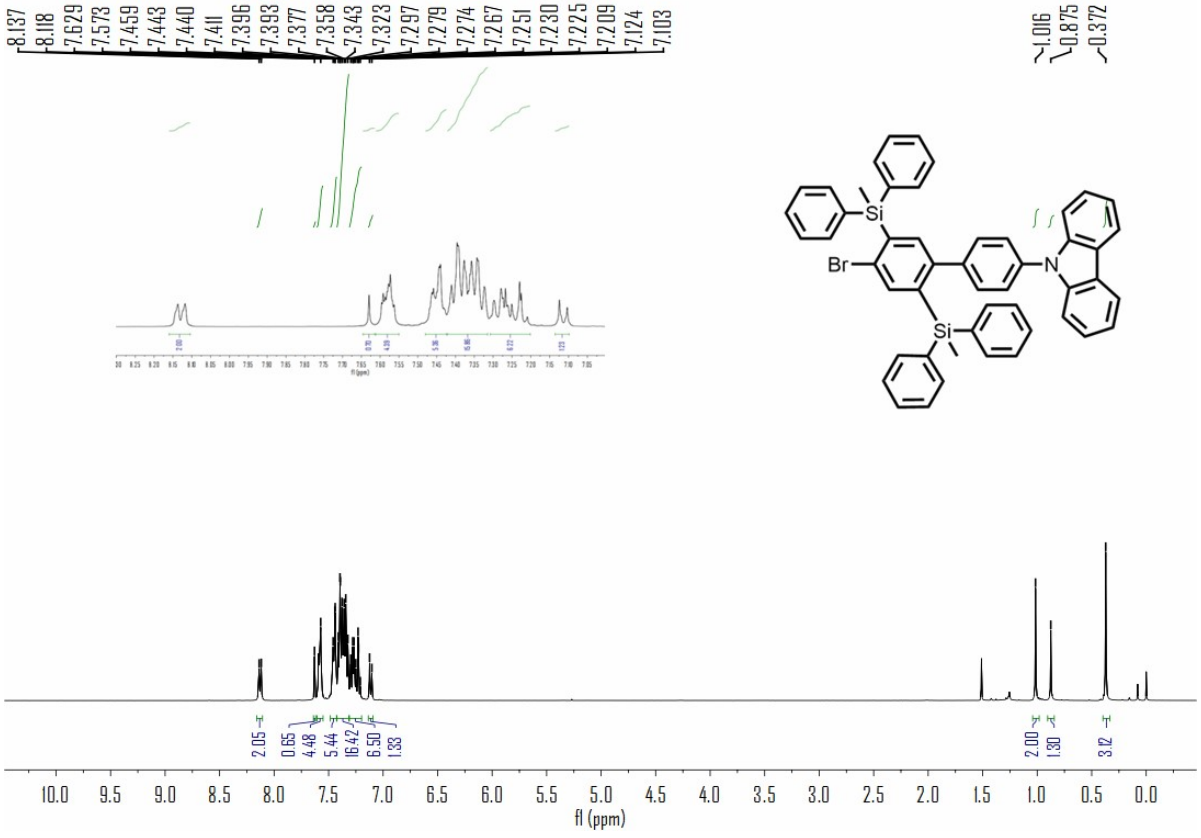
8.137
8.118
7.629
7.573
7.459
7.443
7.440
7.411
7.396
7.393
7.377
7.358
7.343
7.323
7.297
7.279
7.274
7.267
7.251
7.230
7.225
7.209
7.124
7.103
1.016
0.875
0.372
Si
Br
N
Si
2.05
0.65
4.48
5.44
16.42
6.50
1.33
2.00
1.30
3.12
10.0 9.5 9.0 8.5 8.0 7.5 7.0 6.5 6.0 5.5 5.0 4.5 4.0 3.5 3.0 2.5 2.0 1.5 1.0 0.5 0.0
f1 (ppm)

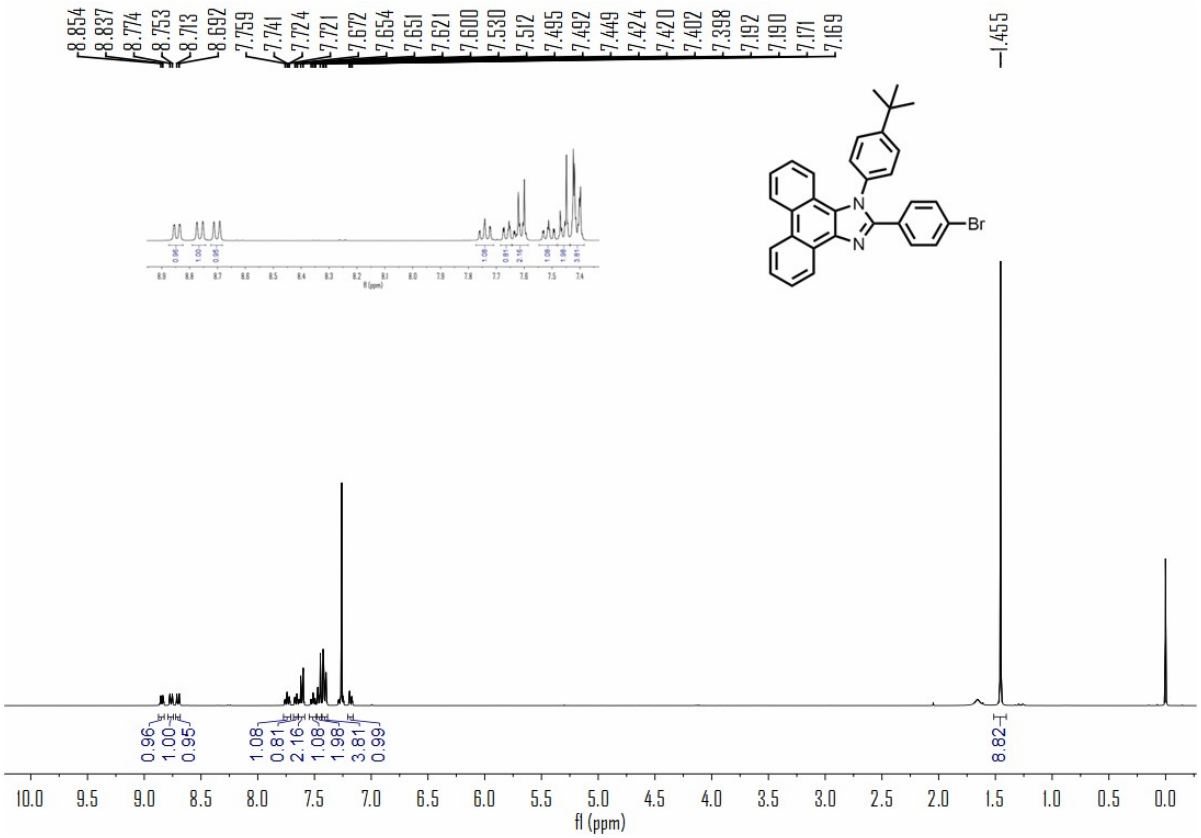
8.854
8.837
8.774
8.753
8.713
8.692
7.759
7.741
7.724
7.721
7.672
7.654
7.651
7.621
7.600
7.530
7.512
7.495
7.492
7.449
7.424
7.420
7.402
7.398
7.192
7.190
7.171
7.169
1.455
Br
N
N
0.96
1.00
0.95
1.08
0.81
2.16
1.08
1.98
3.81
0.99
8.82
10.0
9.5
9.0
8.5
8.0
7.5
7.0
6.5
6.0
5.5
5.0
4.5
4.0
3.5
3.0
2.5
2.0
1.5
1.0
0.5
0.0
f1 (ppm)

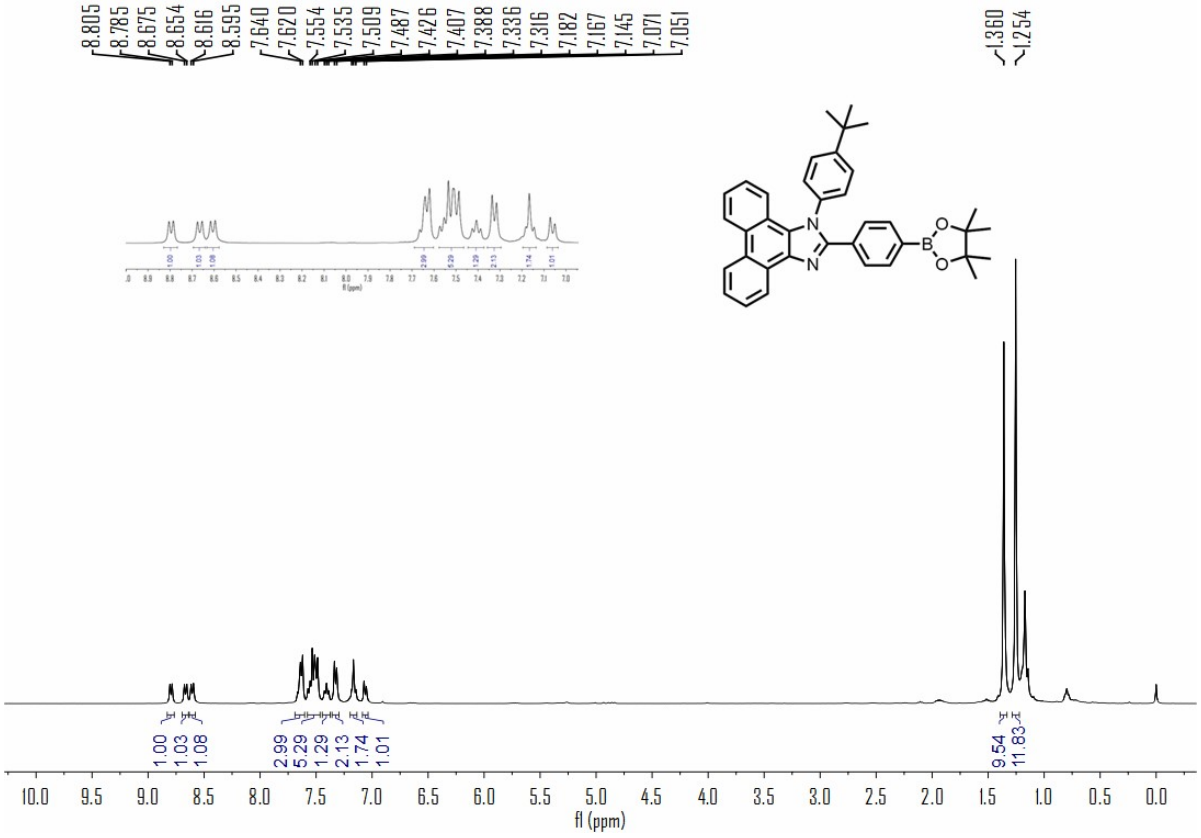
8.805
8.785
8.675
8.654
8.616
8.595
7.640
7.620
7.554
7.535
7.509
7.487
7.426
7.407
7.388
7.336
7.316
7.182
7.167
7.145
7.071
7.051
1.360
1.254
N
N
B
O
O
1.00
1.03
1.08
2.99
5.29
1.29
2.13
1.74
1.01
9.54
11.83
10.0
9.5
9.0
8.5
8.0
7.5
7.0
6.5
6.0
5.5
5.0
4.5
4.0
3.5
3.0
2.5
2.0
1.5
1.0
0.5
0.0
f1 (ppm)

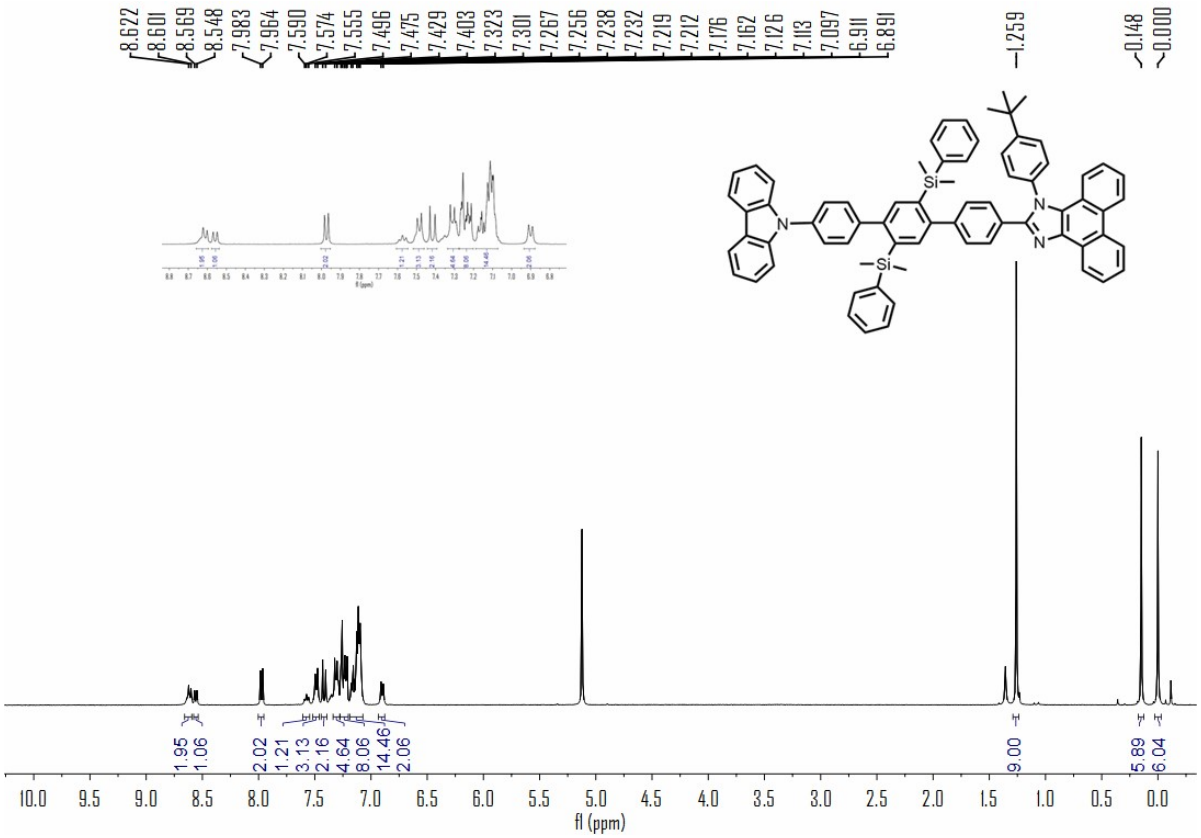
8.622
8.601
8.569
8.548
7.983
7.964
7.590
7.574
7.555
7.496
7.475
7.429
7.403
7.323
7.301
7.267
7.256
7.238
7.232
7.219
7.212
7.176
7.162
7.126
7.113
7.097
6.911
6.891
1.259
0.148
0.000
1.95
1.06
2.02
1.21
3.13
2.16
4.64
8.06
14.46
2.06
9.00
5.89
6.04
f1 (ppm)

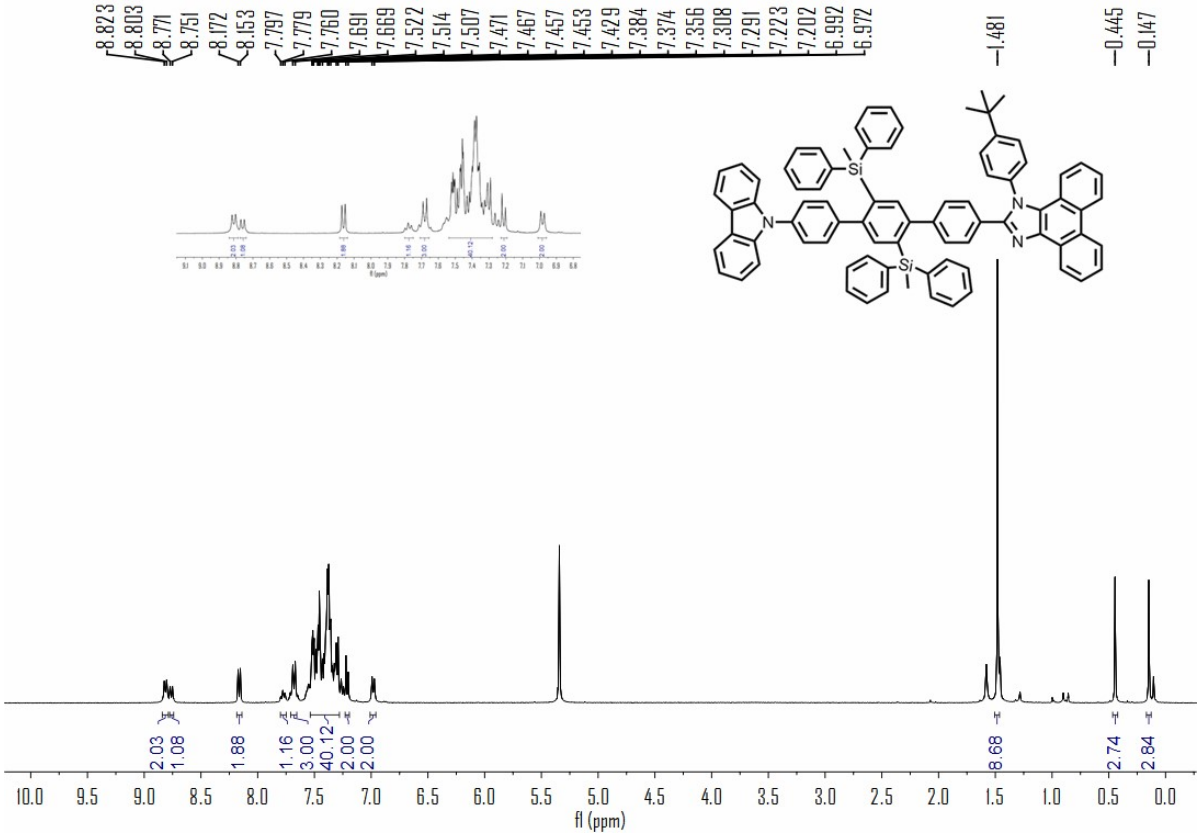
8.823
8.803
8.771
8.751
8.172
8.153
7.797
7.779
7.760
7.691
7.669
7.522
7.514
7.507
7.471
7.467
7.457
7.453
7.429
7.384
7.374
7.356
7.308
7.291
7.223
7.202
6.992
6.972
1.481
0.445
0.147
2.03
1.08
1.88
1.16
3.00
40.12
2.00
2.00
8.68
2.74
2.84
f1 (ppm)

IV. **^{13}C NMR** of **C2MPI** and **C2PPI** in $CDCl_3$ or CD_2Cl_2.

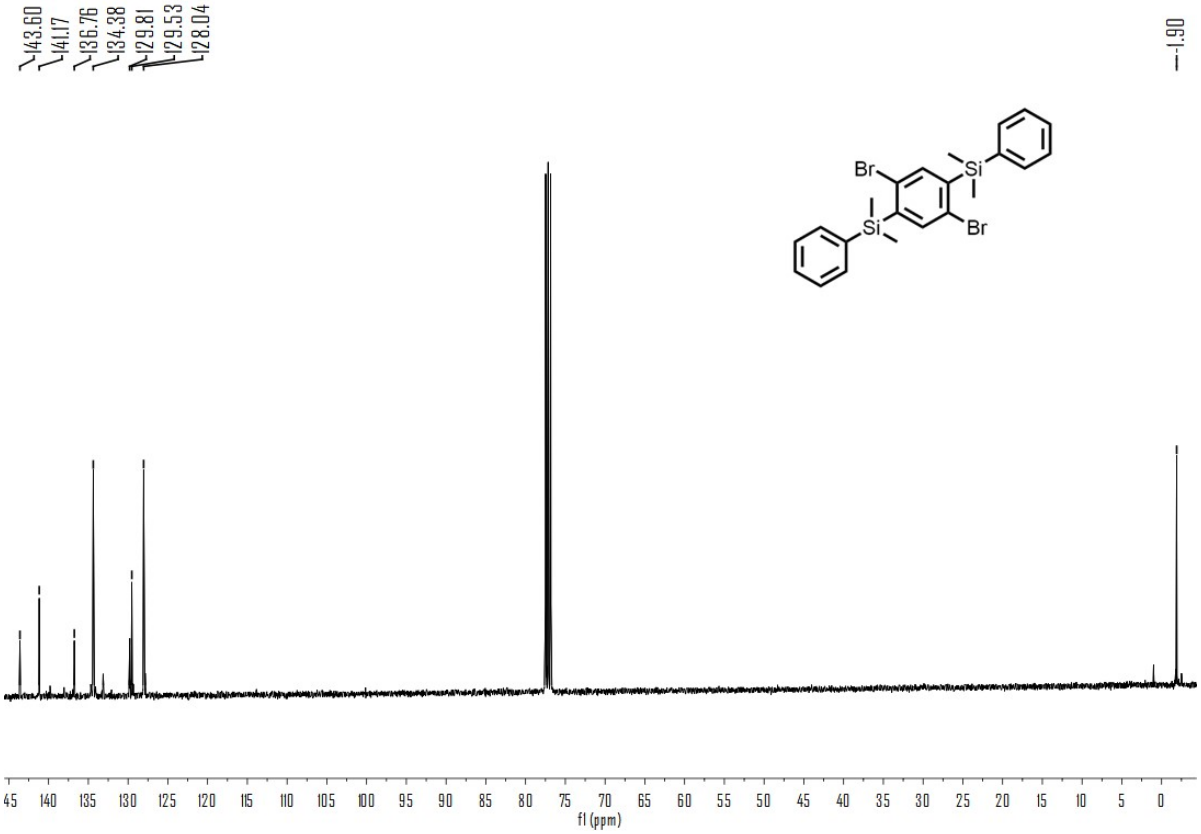

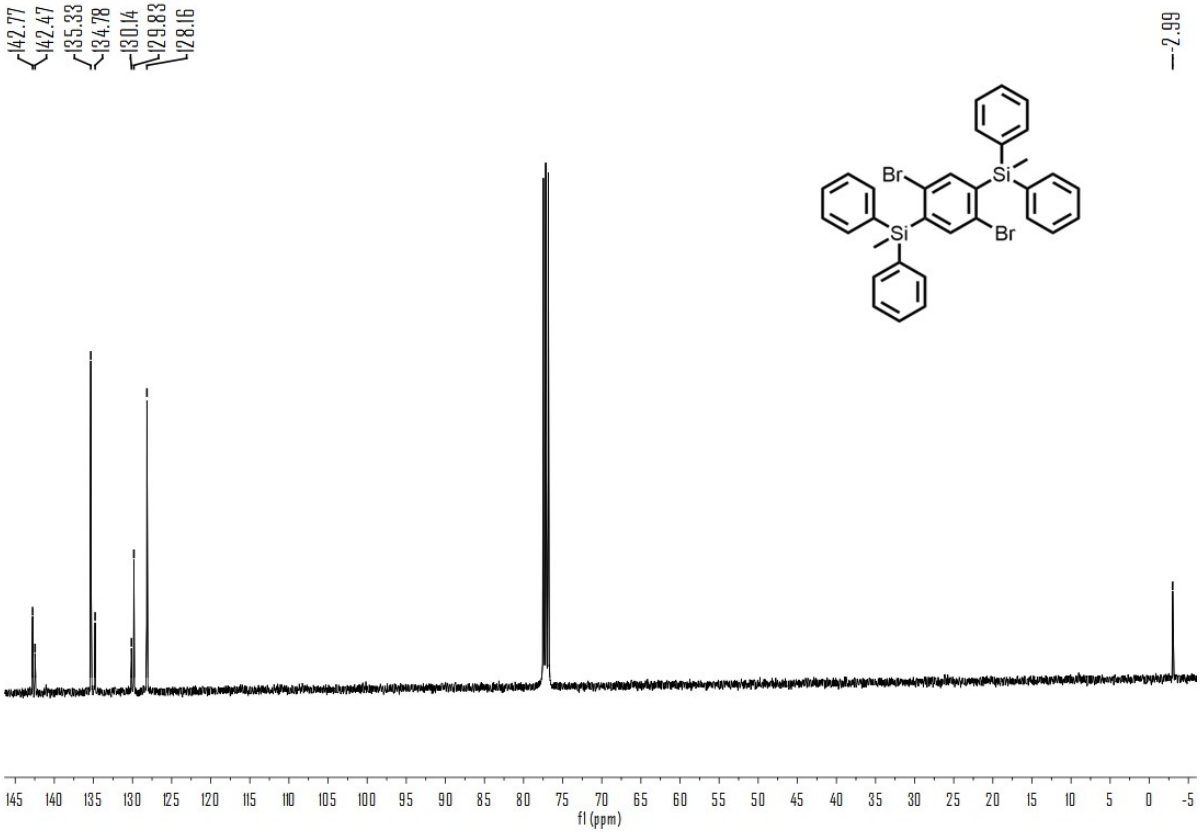

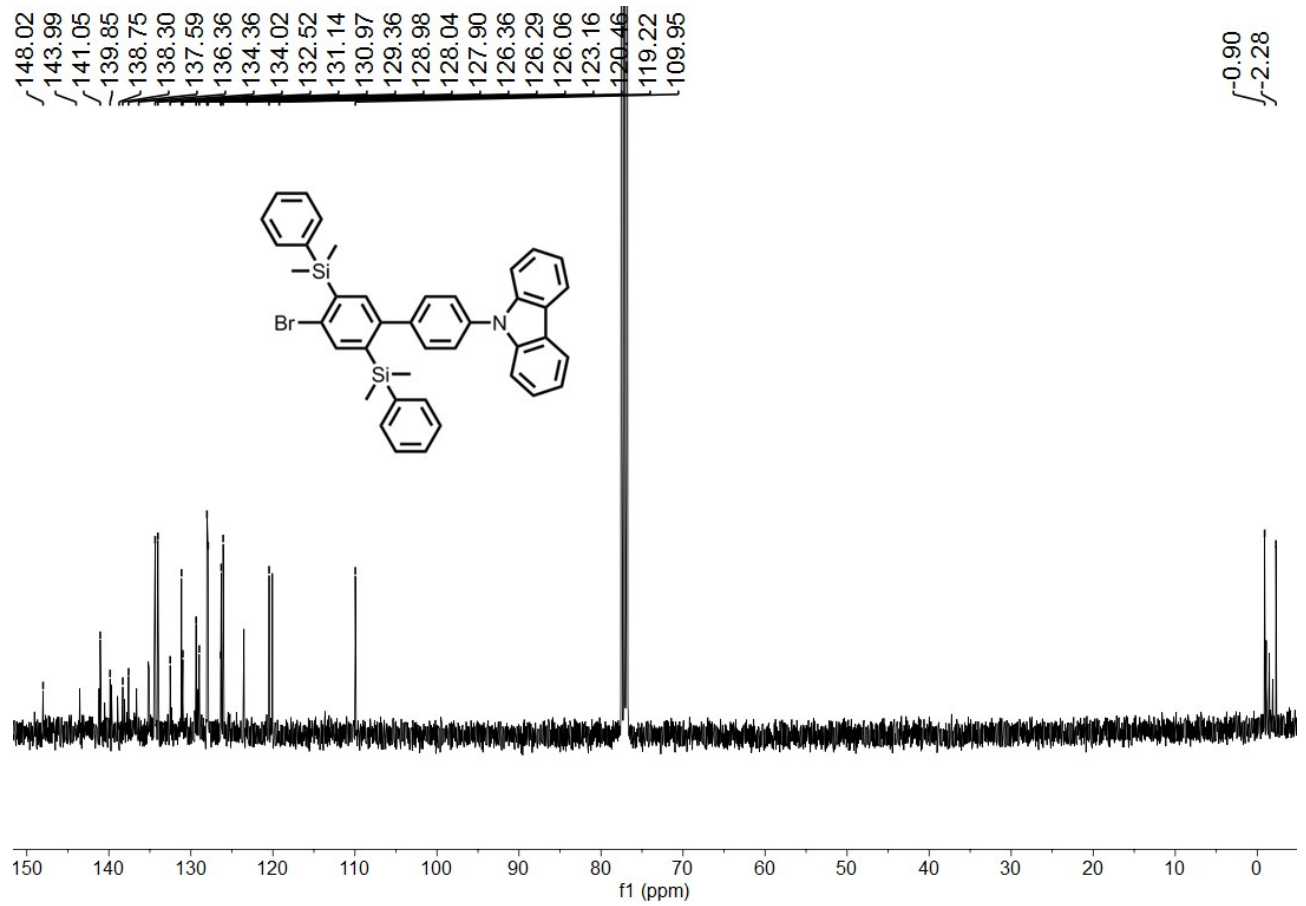
148.02
143.99
141.05
139.85
138.75
138.30
137.59
136.36
134.36
134.02
132.52
131.14
130.97
129.36
128.98
128.04
127.90
126.36
126.29
126.06
123.16
120.46
119.22
109.95
0.90
2.28
Si
Br
N
Si
150
140
130
120
110
100
90
80
70
60
50
40
30
20
10
0
f1 (ppm)

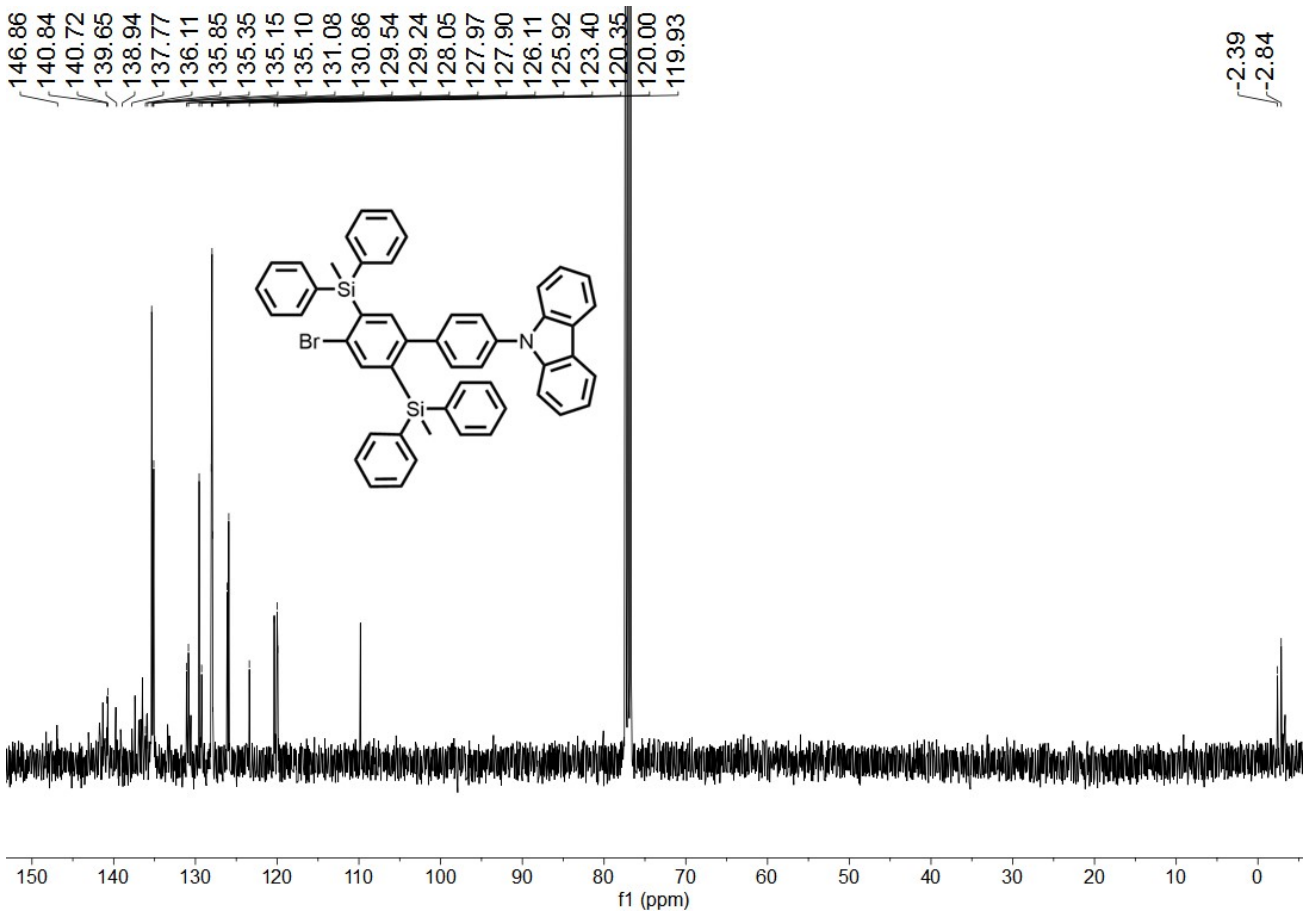
146.86
140.84
140.72
139.65
138.94
137.77
136.11
135.85
135.35
135.15
135.10
131.08
130.86
129.54
129.24
128.05
127.97
127.90
126.11
125.92
123.40
120.35
120.00
119.93
2.39
2.84
Si
Br
N
Si
150
140
130
120
110
100
90
80
70
60
50
40
30
20
10
0
f1 (ppm)

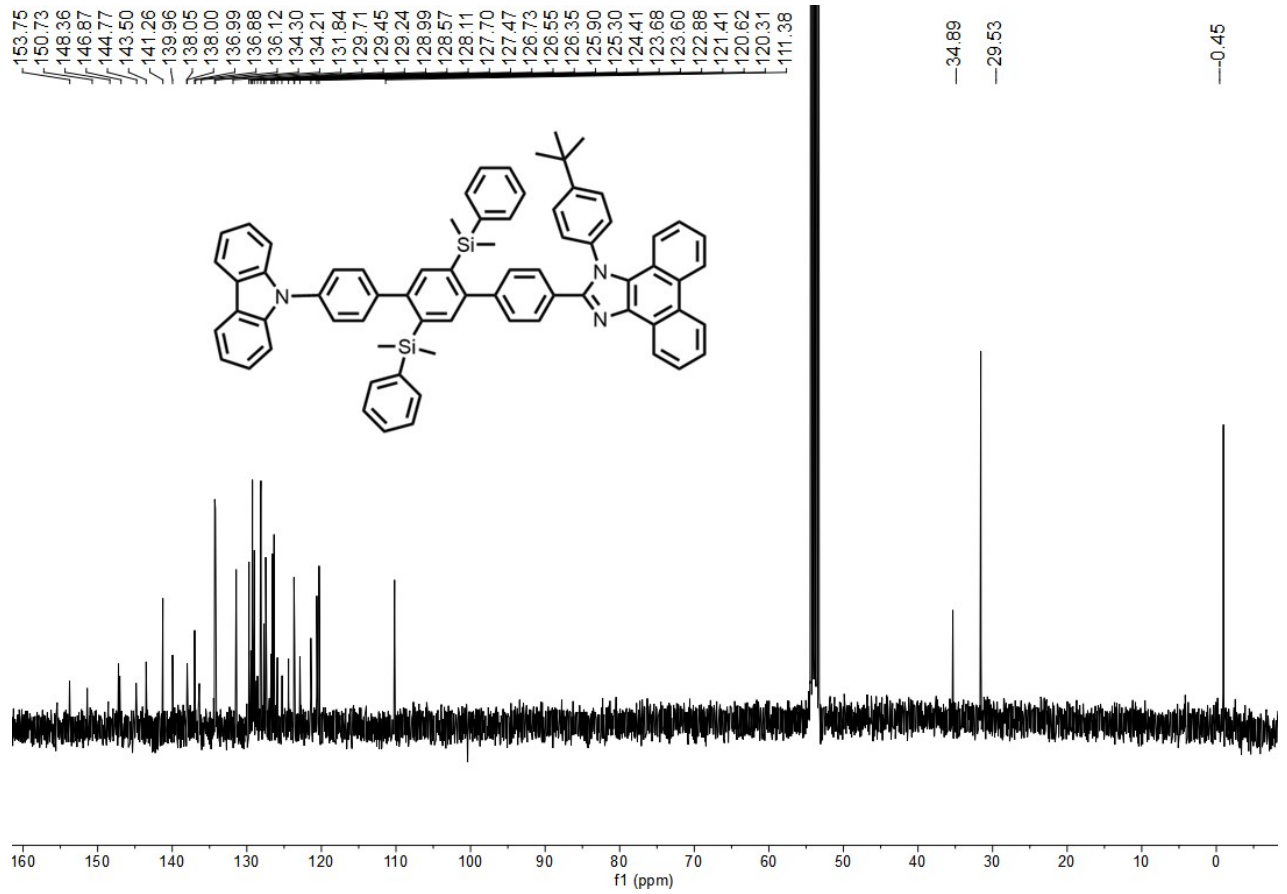
153.75
150.73
148.36
146.87
144.77
143.50
141.26
139.96
138.05
138.00
136.99
136.88
136.12
134.30
134.21
131.84
129.71
129.45
129.24
128.99
128.57
128.11
127.70
127.47
126.73
126.55
126.35
125.90
125.30
124.41
123.68
123.60
122.88
121.41
120.62
120.31
111.38
34.89
29.53
0.45
Si
Si
N
N
N
160
150
140
130
120
110
100
90
80
70
60
50
40
30
20
10
0
f1 (ppm)

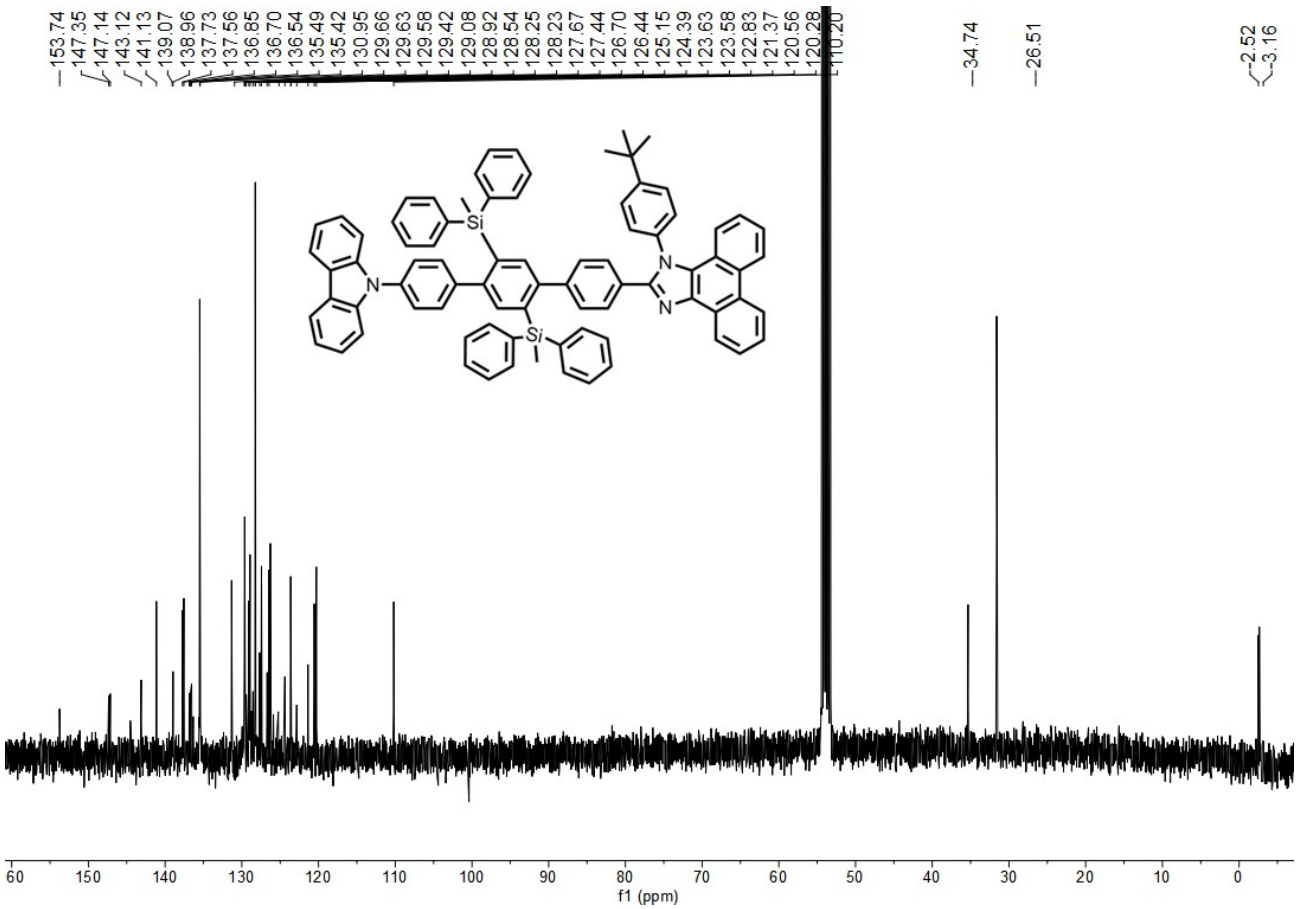
153.74
147.35
147.14
143.12
141.13
139.07
138.96
137.73
137.56
136.85
136.70
136.54
135.49
135.42
130.95
129.66
129.63
129.58
129.42
129.08
128.92
128.54
128.25
128.23
127.67
127.44
126.70
126.44
125.15
124.39
123.63
123.58
122.83
121.37
120.56
120.28
110.20
34.74
26.51
2.52
3.16
Si
Si
N
N
N
60
150
140
130
120
110
100
90
80
70
60
50
40
30
20
10
0
f1 (ppm)

V. HR-MS of C2MPI and C2PPI.

Mass Spectrum SmartFormula Report

Analysis Info

Analysis Name	D:\Data\Q-TOF-LUH-210928-LH-ZZT-1a_01.d	Acquisition Date	9/30/2021 2:34:01 PM
Method	ESI+100-800-201112.m	Operator	BDAL@DE
Sample Name		Instrument / Ser#	microTOF-Q II 228888.10 324
Comment			

Acquisition Parameter

Source Type	ESI	Ion Polarity	Positive	Set Nebulizer	2.0 Bar
Focus	Active	Set Capillary	4500 V	Set Dry Heater	180 °C
Scan Begin	500 m/z	Set End Plate Offset	-500 V	Set Dry Gas	4.0 l/min
Scan End	2000 m/z	Set Collision Cell RF	180.0 Vpp	Set Divert Valve	Source

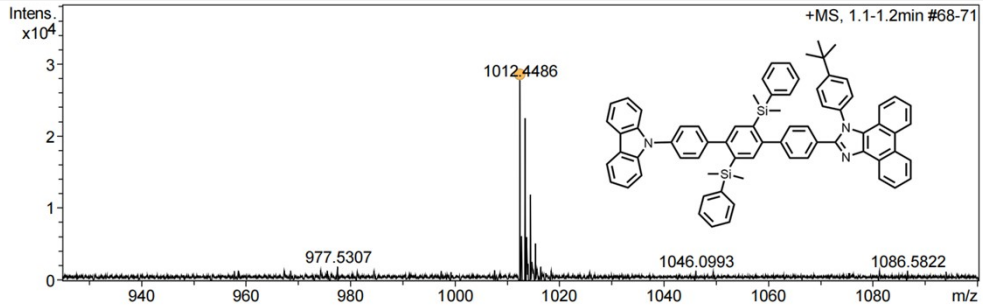

Meas. m/z	#	Ion Formula	m/z	err [ppm]	mSigma	# Sigma	Score	rdb	e⁻ Conf	N-Rule
1012.4486	1	C71H62N3Si2	1012.4477	-0.9	35.8	1	100.00	44.5	even	ok

Mass Spectrum SmartFormula Report

Analysis Info

Analysis Name	D:\Data\Q-TOF-LUH-210928-LH-ZZT-1b_01.d	Acquisition Date	9/30/2021 2:36:12 PM
Method	ESI+100-800-201112.m	Operator	BDAL@DE
Sample Name		Instrument / Ser#	microTOF-Q II 228888.10 324
Comment			

Acquisition Parameter

Source Type	ESI	Ion Polarity	Positive	Set Nebulizer	2.0 Bar
Focus	Active	Set Capillary	4500 V	Set Dry Heater	180 °C
Scan Begin	500 m/z	Set End Plate Offset	-500 V	Set Dry Gas	4.0 l/min
Scan End	2000 m/z	Set Collision Cell RF	180.0 Vpp	Set Divert Valve	Source

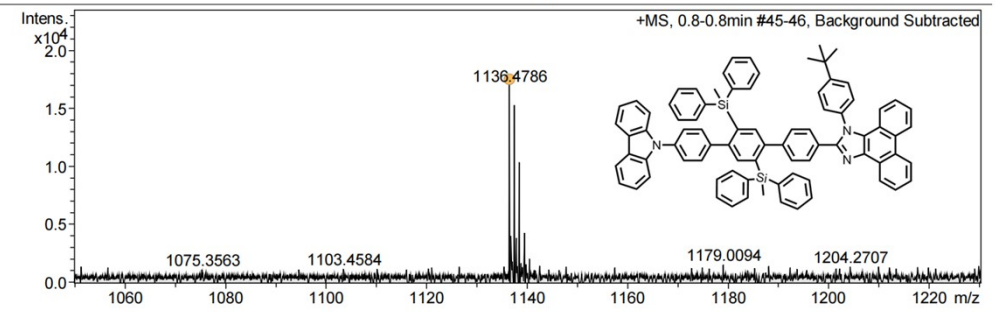

Meas. m/z	#	Ion Formula	m/z	err [ppm]	mSigma	# Sigma	Score	rdb	e⁻ Conf	N-Rule
1136.4786	1	C81H66N3Si2	1136.4790	0.3	60.1	1	100.00	52.5	even	ok